Manifestation of zero-point quantum fluctuations in atomic force microscopy

U. Hartmann

*Institute for Thin Film and Ion Technology, Forschungszentrum Jülich,
D-5170 Jülich, Federal Republic of Germany*
(Received 3 October 1989)

Based on rigorous quantum-field theory, long-range probe-sample dispersion forces in atomic force microscopy are analyzed. The interactions, being attractive or repulsive, can be divided into a purely geometrical part, depending on probe geometry and working distance, and a solely material-dependent part given in terms of the dielectric permittivities involved. The calculations are consistent with published experimental data and promise new analytical possibilities opened by "dispersion microscopy."

The various scanning probe techniques developed from scanning tunneling microscopy[1] ultimately permit the local study of quantum-mechanical phenomena. The underlying quantum-mechanical scale of the actual investigation, however, depends on the physical quantity which is probed. In scanning tunneling microscopy (STM),[2] the tunneling current between two atoms embedded in an environment created by all other atoms is sensed. In spite of the collective origin of the local density of states and the effective barrier height ultimately determining the actual tunneling current, we can consider STM as a technique for analyzing quantum-mechanical phenomena on a microscopic scale. However, if we look at the sum of the individual tunneling events as adding up to the tunneling current, each electron is subjected to an effective capacitance manifesting itself between sample and STM probe. This capacitance is not determined by the macroscopic geometry of the tip-sample arrangement, but rather by the propagation width of the electromagnetic field during one tunneling event. The obtained capacitance values are typically in the 10^{-19} F range and are orders of magnitude smaller than the macroscopic probe-sample stray capacitance.[3,4] The resulting "Coulomb blockade of tunneling" can thus be considered as a mesoscopic quantum-mechanical phenomenon: Upon imaging local variations of the Coulomb blockage, the obtained spatial resolution amounts to some lattice constants.[3]

Atomic force microscopy (AFM) (Ref. 5) locally probes interatomic forces between sample and microtip. Since, unlike STM, this technique does not rely on material conductance, it is the most generally applicable tool for high-resolution surface analysis. The probe-to-sample distance can be varied between a few angstroms up to about 100 nm. Consequently, the range of quantum-mechanical phenomena is completely covered from the microscopic up to the macroscopic scale: Within the tunneling regime, i.e., up to probe-to-sample distances of about 1 nm, wave-function overlap leads to considerable interatomic forces.[6-10] In this microscopic range AFM has produced atomic resolution on some layered materials.[11-16]

However, increasing the AFM working distance beyond the tunneling regime, interaction is solely based on long-range van der Waals force.[12,17-20] The underlying quantum-mechanical scale turns to be a mesoscopic one and, upon reaching a few nanometers working distance, to a macroscopic one. Forces in this regime have been unspecifically attributed to a $-cd^{-n}$ law with $n=6$ or 7 for the interaction potential between two individual atoms of probe and sample and a positive constant c. The present contribution is focused on a rigorous treatment of the problem using methods of quantum-field theory on a mesoscopic as well as macroscopic level.

It is well known that the instantaneous moments of otherwise nonpolar atoms induce polarity in neighboring atoms to give an attractive force. The fluctuations involved are in the uv range and play an important role in optical dispersion. The forces arising from this phenomenon are known as van der Waals dispersion forces. For interatomic separations of more than about 1 nm, dipole interactions generally exceed dipole-quadrupole and higher multipole interactions. In the absence of chemical binding, electrostatic, and magnetostatic forces, dispersion forces are the sole forces between atoms and molecules. They are usually attractive but in special circumstances they can be repulsive.

In a first microscopic approach we look at the interaction between any two isolated atoms of the sample and the AFM probe. In this two-body approach we can restrict ourselves to rudimentary quantum electrodynamics. Based on some well-known classical results,[21] we treat the problem in terms of zero-point perturbations of the two atoms:

$$H = H_{12} + Q_{12} + R_{12} . \tag{1}$$

The total Hamiltonian of the two-body problem is determined by the free-space Hamiltonian of the two atoms H_{12}, by the electrostatic term Q_{12}, and by a term R_{12} describing the interaction of the two atoms with the quantized radiation field. Treating $Q_{12} + R_{12}$ as perturbation operator and applying proper fourth-order perturbation theory we arrive at Casimir's classical result[21] for the interaction energy:

$$U(z)=-\frac{4c}{\hbar z^2}\sum_{l,m}\omega_l\omega_m(q_lq_m)^2\int_0^{\infty}dx\frac{\exp(-2xz)}{(\omega_l^2+c^2x^2)(\omega_m^2+c^2x^2)}\left[x^4+\frac{2x^3}{z}+\frac{5x^2}{z^2}+\frac{6x}{z^3}+\frac{3}{z^4}\right].$$ (2)

The zero state of the atoms is assumed to be a state with the angular momentum $J=0$. Each term in the sum over l,m represents a contribution of the threefold-degenerate states $J=1$. q_i are the respective dipole moments between zero state and the degenerate state, $i=l,m$. ω_i are the corresponding frequencies of the excitations and z denotes the distance between the atoms. The most important feature of this interatomic interaction is given by the limiting cases $z\to0,\infty$:

$$\lim_{z\to0}U(z)=-\frac{3\hbar}{2}\left[\sum_{l,m}\frac{\omega_l\omega_m}{\omega_l+\omega_m}\alpha_l\alpha_m\right]\frac{1}{z^6},$$ (3a)

$$\lim_{z\to\infty}U(z)=-\frac{23\hbar c}{4\pi}\alpha_{10}\alpha_{20}\frac{1}{z^7},$$ (3b)

where the respective static polarizabilities $\alpha_{10,20}$ are given by the sum over all partial polarizabilities α_i, with $i=l,m$. Equation (3a), reflecting London's classical result,[22,23] characterizes the nonretarded interaction obtained for sufficiently small interatomic distances, while Eq. (3b) yields the limit of a solely retarded interaction resulting for distances z which are long compared to the characteristic fluctuation wavelength $\lambda_i=c/\omega_i$.[21]

Now, proceeding on the level of rudimentary QED, we calculate the AFM problem by straightforward integration of potentials of the type $U(z)=-A/z^6$ and $U(z)=-B/z^7$ for some particular probe-sample arrangements. The material constants A,B are known from literature[24] as the microscopic Hamaker constants. As an intermediate result we obtain the force acting on an
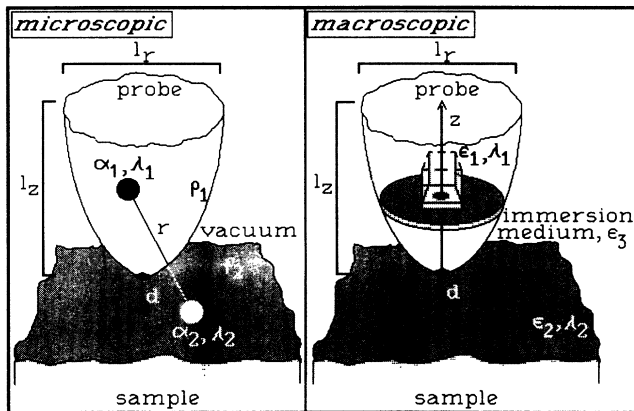
FIG. 1. Schematics of the probe-sample arrangement in AFM. The probe geometry is roughly characterized by the dimensions l_r and l_z, while the sample in a distance d is given by a half space. The atomic material constants (polarizability α, absorption wave length λ, number density ρ, intermediate vacuum) are used in the microscopic approach, while the macroscopic approach is based on the dielectric permittivity ϵ and a macroscopically determined absorption wavelength λ.

individual atom 1 of the AFM probe when the sample is considered as a half space composed of atoms 2 of density ρ_2 (see Fig. 1),

$$f_{nr}(z)=-\frac{\pi}{2}\rho_2\frac{A}{z^4}$$ (4a)

for the nonretarded limit and

$$f_r(z)=-\frac{2\pi}{5}\rho_2\frac{B}{z^5}$$ (4b)

for the solely retarded interaction. To avoid double numerical volume integration of Eq. (2) we subdivide the probe in Fig. 1 into a region near the apex, subjected to a solely nonretarded interaction, and a remaining part, considered to be subjected to a solely retarded interaction with the sample. The transition between these two regimes is defined by $z+d=\lambda$, where z is the vertical coordinate, d the probe-to-sample distance, and $\lambda=\lambda/2\pi$ is a characteristic absorption wavelength determined by both media 1 and 2. In this way the total AFM interaction is given by

$$F(d)=\rho_1\int\int\int_{probe}d^3r[f_{nr}(d+z)+f_r(d+z)],$$ (5a)

with

$$f_r(d+z<\lambda)=0,\quad f_{nr}(d+z>\lambda)=0.$$ (5b)

f_{nr} and f_r are given in Eqs. (4a) and (4b) and ρ_1 denotes the atomic density of the probe.

In the next step we make some reasonable assumptions concerning the AFM probe geometry: AFM probes usually exhibit rotational symmetry.[25] They have a more or less elongated shape with varying sharpness of the apex. To account for these constraints we evaluate Eqs. (5a) and (5b) for a cone representing an ideally sharp tip, a paraboloid modeling a moderately sharp (typical) apex, and a cylinder representing the limit of a completely blunt probe. The results are given by

$$F(d)=-(g_0+g_1d^2+g_2d+g_3/d+g_4/d^2+g_5/d^3)$$ (6a)

for $d<\lambda$, and

$$F(d)=-g_6/d^n$$ (6b)

for the solely retarded interaction regime with $d>\lambda$. The coefficients g_i which are given in a straightforward analytical way by Eqs. (4) and (5) depend on the geometry in terms of l_r,l_z (see Fig. 1) and on the material in terms of $\lambda,A,B,\rho_1,\rho_2$. The result is further simplified due to $g_4=g_5=0$ for the canonical probe, $g_1=g_3=g_5=0$ for the paraboloidal probe, and $g_1=g_2=g_3=g_4=0$ for the cylindrical probe. In the retarded regime, Eq. (6b), we find $n=2$ for the cone, $n=3$ for the paraboloid, and $n=4$

for the cylinder. A semiquantitative impression of the resulting interaction is provided by Fig. 2, where we have assumed a probe-sample arrangement composed of one sort of atom with only one excited state yielding a contribution of $\hbar c/\lambda$ to the London energy.

The assumption of simple pairwise additivity inherent to the above microscopic approach, and, in particular, the definition of the Hamaker constants A and B, ignore the influence of neighboring atoms on the interaction between any pair of probe and sample atoms. Second, the two-body dispersion approach ignores the influence of a third medium usually present between probe and sample in AFM. The existence of multiple reflections of the electromagnetic field in the gap between probe and sample is a further instance where straightforward additivity breaks down. The problems involved in the microscopic approach are completely avoided if we leave the level of rudimentary QED and turn to the macroscopic Lifshitz theory,[26,27] where atomic structure is ignored and the forces between large bodies, now treated as continuous media, are derived in terms of their bulk dielectric properties as shown in Fig. 1.

The basic Lifshitz equation for the interaction per unit surface area of two dielectric half spaces (dielectric permittivities ϵ_1, ϵ_2) separated by a third medium (ϵ_3) of extension z reads[27]

$$f(z) = \frac{\hbar}{4\pi^2 c^3} \int_0^\infty \int_1^\infty p^2 \xi^3 \epsilon_3^{3/2}$$

$$\times \left[\frac{1}{t_1 \exp(x) - 1} + \frac{1}{t_2 \exp(x) - 1} \right] dp \, d\xi , \qquad (7)$$

with $t_1 = (s_1 + p)(s_2 + p)/(s_1 - p)(s_2 - p)$, $t_2 = [s_1 + (\epsilon_1/\epsilon_3)p][s_2 + (\epsilon_2/\epsilon_3)p]/[s_1 - (\epsilon_1/\epsilon_3)p][s_2 - (\epsilon_2/\epsilon_3)p]$, $s_{1,2} = [(\epsilon_{1,2}/\epsilon_3) + p^2 - 1]^{1/2}$, $x = (2p\xi\epsilon_3^{1/2}/c)z$. The dielectric permittivities ϵ are real functions of the imaginary frequencies $\omega = i\xi$ and are the only quantities related to material properties. $\epsilon(\omega)$ is determined in the usual way to

$$\epsilon(\omega) = \epsilon'(\omega) + \epsilon''(\omega) , \qquad (8a)$$

where ϵ'' gives the frequency-dependent dissipation of energy. The real permittivity $\epsilon(i\xi)$ is then given by the Kramers-Kronig relation

$$\epsilon(i\xi) - 1 = \frac{2}{\pi} \int_0^\infty d\omega \frac{\omega \epsilon''(\omega)}{\xi^2 + \omega^2} . \qquad (8b)$$

Thus, the AFM probe-sample interaction is determined, if the permittivity functions $\epsilon''(\omega)$ are given. The latter are conveniently obtained by analysis of reflection measurements. Equation (7) permits, in principle, the calculation of the distance-dependent AFM interaction obtained for any irregularly shaped probe by proper numerical finite-element integration of $f(z)$. The macroscopic
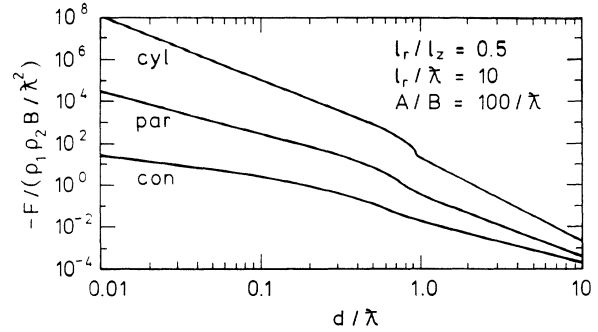
FIG. 2. Probe-sample interaction in AFM according to the microscopic approach. F denotes the force, λ the atomic absorption wavelength, $\rho_{1,2}$ the atomic number densities of probe and sample, and d the probe-to-sample distance. The curves yield a comparison of the force variations for a completely blunt probe (cylindrical), a moderately sharp (typical) probe (paraboloidal), and an ideally sharp probe (conical). For simplicity, probe and sample are assumed to consist of identical materials exhibiting only one excited quantum-mechanical state.

formula (7) directly corresponds to the microscopic approach characterized by Eq. (2).[28,29] A closer comparison between both approaches confirms that the microscopic formulas (4a), (4b), (5a), and (5b) are valid within the framework of continuum theory if the Hamaker constants A, B are calculated in a macroscopically modified way. It should be pointed out that, consequently, the distance dependence obtained from the atomic theory for different AFM probes, Eqs. (6a) and (6b), remains valid with only macroscopically modified coefficients g_i.

To extract the macroscopic Hamaker constants A^*, B^* to be used in Eqs. (6a) and (6b) instead of the microscopic constants $(\rho_1\rho_2 A)$ and $(\rho_1\rho_2 B)$, we expand Eq. (7) for the limits of solely nonretarded and retarded interaction, respectively. For the nonretarded Hamaker constant we obtain

$$A^* = \frac{3\hbar}{4\pi^3} \sum_{\gamma=1}^\infty \frac{1}{\gamma^3} \int_0^\infty d\xi \left[\frac{\epsilon_1 - \epsilon_3}{\epsilon_1 + \epsilon_3} \right]^\gamma \left[\frac{\epsilon_2 - \epsilon_3}{\epsilon_2 + \epsilon_3} \right]^\gamma . \qquad (9)$$

The higher-order contributions for $\gamma \geq 2$ can be attributed to multiple reflections of the electromagnetic field in the gap between probe and sample. Since the second term is at most one-eighth of the first, it is sufficient for the AFM problem to restrict calculations to the $\gamma = 1$ term.

Further simplifications in the calculation of A^* are obtained if the envolved materials only exhibit one pronounced absorption line. According to the Mahanty-Ninham relation,[30] we find for nonmetals

$$\epsilon(i\xi) = 1 + (n^2 - 1)/(1 - \xi^2/\omega_e^2) , \qquad (10a)$$

where ω_e gives the main electronic absorption in the uv (typically 2×10^{16} Hz). n is the refractive index in the visible. Substituting the above result in Eq. (9), we obtain

$$A^* = \frac{3\hbar\omega_e}{8\pi^2\sqrt{2}} \frac{(n_1^2 - n_3^2)(n_2^2 - n_3^2)}{(n_1^2 + n_3^2)^{1/2}(n_2^2 + n_3^2)^{1/2}[(n_1^2 + n_3^2)^{1/2} + (n_2^2 + n_3^2)^{1/2}]} , \qquad (10b)$$

where all three media are assumed to exhibit the same ω_e. On the other hand, the permittivity of a metal is generally given by

$$\epsilon(i\xi)=1+\omega_e^2/\xi^2 \qquad (11a)$$

with the plasma frequency ω_e of the free electron gas [typically $(2-3)\times 10^{16}$ Hz]. With Eq. (9) we obtain

$$A^*=(3/16\pi^2\sqrt{2})\hbar\omega_e \qquad (11b)$$

for the nonretarded interaction between metal probe and sample. Schemes for computing A^* for more complicated absorption spectra are given in the literature.[31-35]

For the solely retarded limit, we find from Eq. (7)

$$B^* = \frac{\pi\hbar c}{24}\frac{\Phi(\epsilon_{10},\epsilon_{20},\epsilon_{30})}{\epsilon_{30}^{1/2}} , \qquad (12a)$$

where the subscript "0" indicates the fact that B^* only depends on the respective static dielectric constants in terms of a function Φ, given by

$$\Phi(\epsilon_{10},\epsilon_{20},\epsilon_{30})=\frac{15}{2\pi^4}\int_0^\infty\int_1^\infty\frac{x^3}{p^2}\left[\frac{1}{t_{10}\exp(x)-1}\right]$$
$$\times\left[\frac{1}{t_{20}\exp(x)-1}\right]dp\,dx , \qquad (12b)$$

where $t_{10,20}$ are given in connection with Eq. (7). It is reasonable to derive some simplifications of Eq. (12b) relevant to AFM: If probe and sample consist of materials with low static dielectric constants (≤ 5), we find

$$\Phi(\epsilon_{10},\epsilon_{20},\epsilon_{30})=\frac{69}{2\pi^4}\sum_{\gamma=1}^\infty\frac{1}{\gamma^4}\left[\frac{\epsilon_{10}-\epsilon_{30}}{\epsilon_{10}+\epsilon_{30}}\right]^\gamma\left[\frac{\epsilon_{20}-\epsilon_{30}}{\epsilon_{20}+\epsilon_{30}}\right]^\gamma , \qquad (13)$$

where, as in Eq. (9), the contributions for $\gamma\geq 2$ result from multiple reflections in the gap and can generally be neglected. For two identical dielectric materials $\epsilon_{10}=\epsilon_{20}=\epsilon_0$ and for a metal-dielectric ensemble $\epsilon_{10}\to\infty,\epsilon_{20}=\epsilon_0$, the respective values of $\Phi(\epsilon_0)$ are given in Fig. 3. For the particular case of two metals, we simply obtain $\Phi=1$. The latter result confirms that the retarded AFM contribution does not in any way depend on the nature of the metals employed for probe and sample. This is certainly not the case for the nonretarded contribution given in Eq. (9).

Substituting the dispersion relation (11a) into Eq. (7), we have calculated the AFM probe-sample force obtained for a sole metal ensemble at intermediate vacuum. Numerical integration yields the curves shown in Fig. 4(a) for a blunt, a moderately sharp, and an ideally sharp probe, respectively. The inset shows additionally the abrupt-transition approximation obtained with Eqs. (6a) and (6b) using the macroscopic Hamaker constants A^* from Eq. (11b) and B^* from Eq. (12a), with $\Phi=1$. Addi-
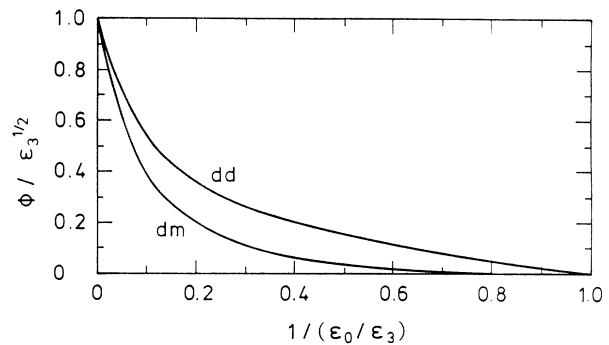
FIG. 3. Permittivity functions determining the retarded Hamaker constant if AFM probe and sample consist of identical dielectrics with permittivity ϵ_0 (dd) or of a metal $(\epsilon_0\to\infty)$-dielectric (ϵ_0) ensemble (dm).
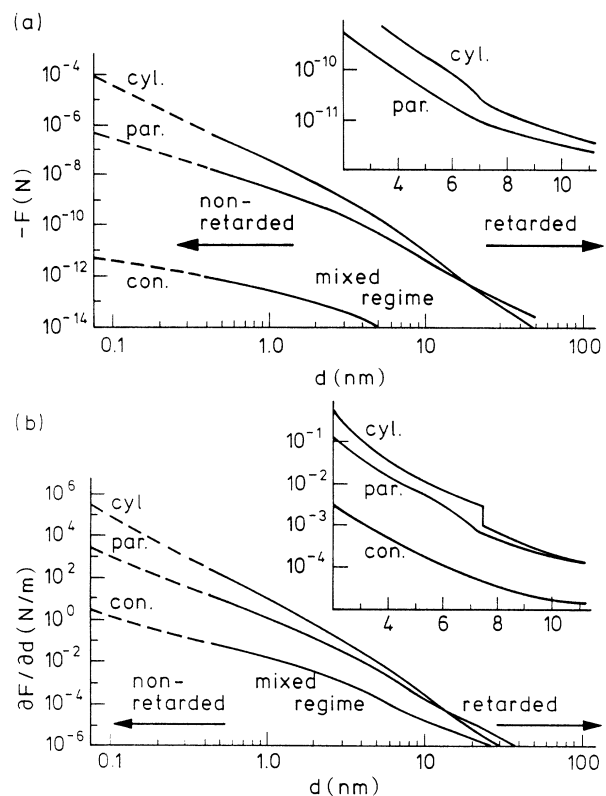
FIG. 4. AFM probe-sample interactions for a metal-metal arrangement at intermediate vacuum, calculated for some typical probe geometries: for a completely blunt (cylindrical, $l_r=470$ nm), a moderately sharp (paraboloidal, $l_r/l_z=0.5$, $l_r=47$ μm), and an ideally sharp (conical, $l_r/l_z=0.5$) tip. (a) shows the force variations calculated rigorously by numerical integration of the Lifschitz equation. The simple analytical approximation obtained by the abrupt-transition approach is given in the inset. (b) shows the corresponding compliance curves measurable in most AFM devices. The abrupt-transition approach exhibits a discontinuity at a probe-to-sample distance of $d=\chi$, where $\chi=\lambda/2\pi$ is the plasma wavelength of the metals. The latter has been representatively assumed as 47 nm. The curves can be subdivided into a solely nonretarded regime close to tunneling distances, a mixed regime around $d=\chi$, and a solely retarded regime for large distances. Within the tunneling regime (dashed lines), wave-function overlap leads to additional contact forces not evolved in the present theory.

tionally we have calculated the resulting probe-sample compliance $\partial F/\partial d$ in Fig. 4(b), which is sensed in many AFM experiments rather than the force. The inset clearly shows, at least for the cylindrical probe, the discontinuity resulting from the abrupt-transition approach if the probe-to-sample distance equals the absorption wavelength of the metals. On the other hand, comparison between the exact curves and the simple analytical approximation, subdividing the probe into volume element of solely nonretarded and retarded interactions, confirms the satisfactory accuracy obtained when using A^*, B^* in connection with Eqs. (6a) and (6b).

Finally some general consequences of the above theory should be summarized. (i) The dispersion force measured in vacuum is always attractive. (ii) The force is always attractive if probe and sample consist of the same material, while it can be attractive or repulsive for different materials. A repulsion is obtained if the intermediate medium exhibits an effective refractive index lying in between that of probe and sample, e.g., $n_1 < n_3 < n_2$. (iii) The AFM force remains unchanged if probe and sample materials are exchanged.

Additionally, it should be pointed out that thin adsorption or oxide layers on AFM probe and sample have a marking influence on the obtained dispersion forces. For only a few monolayers they can dominate the interactions, even leading to a change in sign of the force. In general, the effect of surface contaminations depends on the actual probe-to-sample distance and complicates interpretation of the experimental results.[36]

In conclusion, we have shown by a rigorous quantum-electrodynamical approach that the long-range interactions, obtained in AFM beyond the tunneling regime, are given by van der Waals dispersion forces for an electrically neutral and nonmagnetic probe-sample arrangement. The decay of force with increasing working distance cannot be characterized by a simple $-cd^n$ law with $c > 0$ and $n < 0$. The distance dependence is rather approximately given by a linear combination of such terms with n generally reaching from -4 to 2 and c being positive, zero, or negative, respectively, depending on the actual probe geometry and on the material parameters involved. In this way, "dispersion microscopy" can lead to attractive or repulsive interactions being strongly influenced by surface contaminations. The quantitative results are consistent with experimental data published up to the present time.[12,17-20] In particular, the occasionally observed repulsive interactions[37] are clearly explained.

When scanning the probe across the sample and working in the usual constant-response mode, the AFM does not simply trace the surface topography, but rather traces profiles of constant dielectric response. This is in analogy to the usual STM mode of tracing a profile of constant local density of states. In this way dispersion microscopy can provide important information on the dielectric response of various media in terms of their Hamaker constants and characteristic adsorption wavelengths. This consequence has been completely ignored in the literature up to the present time.

In the latter context it is important that the AFM interaction changes with increasing working distance, by starting from the tunneling regime, from a solely nonretarded over a mixed regime to a solely retarded regime. This behavior is clearly emphasized by a simple analytical approximation based on a subdivision of the probe into volume elements, either exhibiting a solely nonretarded or retarded interaction with the sample. This simple approximation turns out to be satisfactory in all practical cases and permits an easy calculation of the respective AFM response for any given material, probe geometry, and working distance.

---

[1]For an extensive review, see Y. Kuk and P. J. Silverman, Rev. Sci. Instrum. **60**, 165 (1989).

[2]G. Binnig and H. Rohrer, Rev. Mod. Phys. **59**, 615 (1987).

[3]U. Hartmann (unpublished).

[4]P. J. M. van Bentum, H. van Kempen, L. E. C. van de Leemput, and P. A. A. Teunissen, Phys. Rev. Lett. **60**, 2543 (1988).

[5]G. Binnig, C. F. Quate, and Ch. Gerber, Phys. Rev. Lett. **56**, 930 (1986).

[6]J. H. Rose, J. Ferrante, and J. R. Smith, Phys. Rev. Lett. **47**, 675 (1987).

[7]J. Ferrante and J. R. Smith, Phys. Rev. B **31**, 3427 (1985).

[8]D. H. Buckley, J. Ferrante, M. D. Pashley, and J. R. Smith, Mater. Sci. Eng. **83**, 177 (1986).

[9]J. B. Pethica and W. C. Oliver, Phys. Scr. **T19**, 61 (1987).

[10]M. Dürig, O. Züger, and D. W. Pohl, J. Microsc. **152**, 259 (1988).

[11]C. M. Mate, G. M. McCelland, R. Erlandsson, and S. Chiang, Phys. Rev. Lett. **59**, 1942 (1987).

[12]O. Marti, B. Drake, S. Gould, and P. K. Hansma, J. Vac. Sci. Technol. A **6**, 287 (1988).

[13]O. Marti, B. Drake, and P. K. Hansma, Appl. Phys. Lett. **51**, 484 (1987).

[14]G. Binnig, Ch. Gerber, E. Stoll, T. R. Albrecht, and C. F. Quate, Europhys. Lett. **3**, 1281 (1987).

[15]T. R. Albrecht and C. F. Quate, J. Appl. Phys. **62**, 2599 (1987).

[16]T. R. Albrecht and C. F. Quate, J. Vac. Sci. Technol. A **6**, 271 (1988).

[17]R. Erlandsson, G. M. McClelland, C. M. Mate, and S. Chiang, J. Vac. Sci. Technol. A **6**, 266 (1988).

[18]M. Anders and C. Heiden, J. Microsc. **152**, 643 (1988).

[19]H. Iamanda, T. Fuji, and N. Nahayama, J. Vac. Sci. Technol. A **6**, 293 (1988).

[20]Y. Martin, C. C. Williams, and H. K. Wickramasinghe, J. Appl. Phys. **69**, 4723 (1987).

[21]H. B. G. Casimir and D. Polder, Phys. Rev. **73**, 360 (1948).

[22]R. Eisenschitz and F. London, Z. Phys. **60**, 491 (1930).

[23]T. H. Boyer, Phys. Rev. A **6**, 314 (1972).

[24]J. Visser, Adhesion of Colloidal Particles, in Surface and Colloid Science, edited by E. Matijevic (Wiley, New York, 1976).

[25]T. Göddenhenrich, U. Hartmann, M. Anders, and C. Heiden, J. Microsc. **152**, 527 (1988).

[26] E. M. Lifshitz, Zh. Eksp. Teor. Fiz. **29**, 94 (1955) [Sov. Phys.—JETP **2**, 73 (1956)].

[27] I. E. Dzyaloshinskii, E. M. Lifshitz, and L. P. Pataevskii, Zh. Eksp. Teor. Fiz. **37**, 229 (1959) [Sov. Phys.—JETP **10**, 161 (1960)].

[28] J. N. Israelachvili, Proc. R. Soc. London, Ser. A **331**, 39 (1972).

[29] J. N. Israelachvili, *Intermolecular and Surface Forces with Applications to Colloidal and Biological Systems* (Academic, London, 1985).

[30] J. Mahanty and B. W. Ninham, *Dispersion Forces* (Academic, New York, 1976).

[31] R. G. Horn and J. N. Israelachvili, J. Chem. Phys. **75**, 1400 (1981).

[32] J. N. Israelachvili, P. M. McGuiggen, and A. M. Homola, Science **240**, 189 (1988).

[33] J. Gregory, Adv. Colloid Interface Sci. **2**, 396 (1970).

[34] R. M. Pashley, Adv. Colloid Interface Sci. **62**, 344 (1977).

[35] D. B. Hough and L. R. White, Adv. Colloid Interface Sci. **14**, 3 (1980).

[36] A complete AFM response theory including the effect of surface contamination layers is planned to be published elsewhere.

[37] M. Anders (private communication).

FIG. 1. Schematics of the probe-sample arrangement in AFM. The probe geometry is roughly characterized by the dimensions l_r and l_z, while the sample in a distance d is given by a half space. The atomic material constants (polarizability α, absorption wave length λ, number density ρ, intermediate vacuum) are used in the microscopic approach, while the macroscopic approach is based on the dielectric permittivity ϵ and a macroscopically determined absorption wavelength λ.